Determination of spray drift and buffer zones in 3D crops using the ISO standard and new LiDAR methodologies

Xavier Torrent[a,*], Eduard Gregorio[a], Joan R. Rosell-Polo[a] , Jaume Arnó[a], Miquel Peris[b], Jan C. van de Zande[c], Santiago Planas[a,d]

[a] Research Group in AgroICT & Precision Agriculture, Department of Agricultural and Forest Engineering, Universitat de Lleida (UdL)-Agrotecnio Center, Lleida, Spain.

[b] Institut de Recerca i Tecnologia Agroalimentària (IRTA), Parc Científic i Tecnològic Agroalimentari, Lleida, Spain.

[c] Wageningen University & Research – Agrosystems Research, Wageningen, The Netherlands.

[d] Plant Health Services, Generalitat de Catalunya, Lleida, Spain.

* Corresponding author. E-mail address: xavier.torrent@eagrof.udl.cat (X. Torrent).

Abstract

Spray drift generated in the application of plant protection products in tree crops (3D crops) is a major source of environmental contamination, with repercussions for human health and the environment. Spray drift contamination acquires greater relevance in the EU Southern Zone due to the crops structure and the weather conditions. Hence, there is a need to evaluate spray drift when treating the most representative 3D crops in this area. For this purpose, 4 spray drift tests, measuring airborne and sedimenting spray drift in accordance with ISO 22866:2005, were carried out for 4 different crops (peach, citrus, apple and grape) in orchards of the EU Southern Zone, using an air-blast sprayer equipped with standard (STN) and spray drift reduction (DRN) nozzle types. A further 3 tests were carried out to test a new methodology for the evaluation of spray drift in real field conditions using a LiDAR system, in which the spray drift generated by different sprayer and nozzle types was contrasted. The airborne spray drift potential reduction (DPR_V) values, obtained following the ISO 22866:2005, were higher than those for sedimenting spray drift potential reduction (DPR_H) (63.82%-94.42% vs. 39.75%-69.28%, respectively). For each crop and nozzle type combination, a sedimenting spray drift model was also developed and

used to determine buffer zone width. The highest buffer width reduction (STN vs DRN) was obtained in peach (>75%), while in grape, citrus and apple only 50% was reached. These results can be used as the starting point to determine buffer zone width in the countries of the EU Southern Zone depending on different environmental threshold values. Tests carried out using LiDAR system demonstrated high capacity and efficiency of this system and this newly defined methodology, allowing sprayer and nozzle types in real field conditions to be differentiated and classified.

Keywords: pesticide spraying, spray drift, light detection and ranging, spray drift potential reduction, hollow-cone nozzles, remote sensing

Nomenclature

DPR	spray drift potential reduction (%)
DPR_H	spray drift potential reduction based on sedimenting drift (%)
DPR_{lidar}	spray drift potential reduction based on LiDAR measurements (%)
DPR_V	spray drift potential reduction based on airborne drift (%)
$DPR_{V(5m)}$	spray drift potential reduction based on airborne drift at 5 m from the center of the last alley of the plot (%)
$DPR_{V(10m)}$	spray drift potential reduction based on airborne drift at 10 m from the center of the last alley of the plot (%)
DRN	spray drift reduction nozzle
DRT	spray drift reduction technique
D_{V50}	volume diameter, indicating that 50% of the spray volume is in smaller droplets (µm)
F_H	sedimenting spray drift based on ISO field measurements (%)
$F_{V(5m)}$	airborne spray drift based on ISO field measurements at 5 m from the center of the last alley of the plot (%)
$F_{V(10m)}$	airborne spray drift based on ISO field measurements at 10 m from the center of the last alley of the plot (%)

HC	hollow-cone
PDPA	phase Doppler particle analyzer
$S_{L(Lab)}$	spray drift potential based on laboratory LiDAR measurements (%)
$S_{L(Field)}$	spray drift based on field LiDAR measurements (%)
STN	standard nozzle
V_{100}	volume fraction of droplets smaller than 100 µm in diameter (%)
V_{200}	volume fraction of droplets smaller than 200 µm in diameter (%)
WT_H	sedimenting spray drift potential based on wind tunnel measurements (%)
WT_V	airborne spray drift potential based on wind tunnel measurements (%)

1. Introduction

The application of plant protection products (PPP) in crops is fundamental for the control of pests and diseases and to ensure agricultural production. According to Eurostat data (2016), Spain was the EU country with the highest consumption of PPP (77 thousand tons), representing 20.9% of total EU consumption, followed by France (72 thousand tons; 19.5%) and Italy (60 thousand tons; 16.3%). In this scenario, spray drift associated with PPP spraying operations is a primary source of contamination. This phenomenon implies a clear risk for the health of bystanders and local residents (dermal exposure and inhalation) and for the environment (air, surface water, ground water, soil, fauna, flora and other crops) (Damalas, 2015; EPA, 2018; EPPO, 2003). These risks have been explored by several authors. Studies by Butler Ellis et al. (2010, 2018) on the exposure of bystanders to PPP airborne spray drift was used for the assessment of relevant UK regulations. Sjerps et al. (2019) analyzed drinking water sources in the Netherlands, identifying the presence of 15 pesticides. De Schampheleire et al. (2007) evaluated spray drift damage to crops in Belgium, concluding that the most extreme risk situations occur in the case of 3D crops (fruit crops). In this regard, Sarigiannis et al. (2013) reported how most pesticide emissions generated in 3D crops are concentrated in Spain and

Italy and that there are major differences between the countries of the EU Southern Zone and those of the Northern Zone as a result of climatic conditions.

One of the most important reasons for quantifying spray drift in 3D crops is to measure its potential reduction through the use of different spray drift reduction techniques (DRT): nozzle type (Derksen et al., 2007), sprayer type (Wenneker et al., 2016), air assistance (Duga et al., 2017), tractor-sprayer forward speed (Lešnik et al., 2015), windbreaks, buffer zones, etc. In this line, the European Directive 2009/128/EC (EU, 2009) for sustainable pesticide use proposes the establishment of buffer zones as a drift reducing measure additional to the DRT. Buffer zones are defined as areas of land that allow the treatment area to be separated from non-target areas in order to mitigate the pollution caused by PPP treatments (Muscutt et al., 1993). In a recent study by Castro-Tanzi et al. (2018), the buffer distances were estimated according to the environmental risk of spray drift. Several studies have been carried out in the north of Europe to determine buffer zones in 2D (field crops) and 3D crops (De Schampheleire et al., 2007; van de Zande et., 2010). However, as far as the authors of the present study are aware, no studies have been conducted to date on adaptation and adjustment of these buffer zones to the crop architecture and environmental conditions typical of the EU Southern Zone.

Spray drift in 3D crops is mainly influenced by the crop to be treated (canopy architecture and porosity, growth stage, etc.) (Da Silva et al., 2006; Kasner et al., 2018), sprayer design (fan characteristics, deflectors, etc.) (Blanco et al., 2019; Salyani et al., 2013), spray mix properties (surface tension, viscosity, etc.) (Stainier et al., 2006), operating conditions (droplet size distribution, liquid volume rate, forward speed, air assistance, etc.) (Nuyttens et al., 2005), and weather conditions (temperature, relative humidity, wind speed and direction, etc.) (Gil et al., 2007). It should be noted that most of the many numerous authors who have conducted spray drift tests in field conditions have only done so in 2D crops (Carlsen et al., 2006; Nuyttens et al., 2010; Wolters et al., 2008). As for the evaluation of spray drift in 3D crops, most of the few studies that have been carried out have focused on citrus (Cunha et al., 2012; Garcerá et al., 2017; Salyani et al., 2013). Recently, Bourodimos et al. (2019) has developed a new spray drift

risk assessment tool (model) for vineyard that has been contrasted with ISO 22866:2005. It should also be noted that carrying out the tests in different scenarios (training system and architecture of crops, meteorological conditions, etc.) can lead to under or overestimations of spray drift, as was demonstrated by Ramos et al. (2000). Spray drift prediction models have been created from numerous tests conducted for spray drift evaluation. The best known in Europe are the German models for 2D and 3D crops based on 50 trials in field crops and 72 in fruit orchard (Ganzelmeier et al., 1995; Rautmann et al., 2001), and the Dutch model for pome fruit trees (apple and pear) based on 20 years of experimental data (Holterman et al., 2017).

Currently, the reference method for the evaluation of spray drift in real field conditions is ISO 22866:2005. However, conducting field spray drift trials based on this standard is very time consuming and laborious. An alternative methodology has been proposed for quantifying spray drift based on LiDAR technology (Gregorio et al., 2014, 2018; Hiscox et al., 2006; Richardson et al., 2017), due to its advantages in terms of measurement capacity (temporal and spatial resolution, real time measurements), as well as its reduced labour and time requirements. Other authors as Gil et al. (2013) have tested low-cost LiDAR sensors obtaining spray drift measurements that were not range-resolved. Another optical remote sensing technique used to evaluate the spray drift is the Open-Path Fourier Transform Infra-Red (OP-FTIR) spectrometry (Kira et al., 2018).

Given all of the above, there is a clear need to know the effect and behavior of spray drift in all the main 3D crops in the EU Southern Zone and to adopt appropriate and effective DRT. Consequently, the first aim of this work is to evaluate spray drift (sedimenting and airborne) for different types of standard (STN) and spray drift reduction nozzles (DRN) in different 3D crops (peach, apple, citrus, grape) in field conditions, using ISO 22866:2005. The second aim is to determine and compare the buffer zones required to minimize the effects of spray drift in the different crop and nozzle types studied. The third aim of this work is to define and perform a preliminary validation of a new methodology to measure spray drift in real field conditions using an ad hoc LiDAR system.

2. Materials and methods

2.1. Sprayer and nozzle characterization

Seven field spray drift tests (T1-T7) were conducted in compliance with ISO 22866:2005 in which STN and DRN hollow-cone nozzles were compared in four 3D crops (peach, citrus, apple and grape). Table 1 shows the characteristics of the orchards and crops, and Table 2 specifies the sprayers and nozzles used in each test and their operating conditions.

The sprayer used in the first test (T1) was a cross-flow air-assisted sprayer (Arrow F-1000, Hardi S.A., Lleida, Spain) with an air flow rate of 65,000 $m^3 \cdot h^{-1}$ and equipped with 20 operating nozzles. The nozzles were standard hollow-cone Albuz ATR 80 Orange (STN-O) (Solcera, Evreux, France) and spray drift reduction hollow-cone Albuz TVI 8002 Yellow (DRN-Y), operating at 1.0 and 0.9 MPa, respectively, with flow rates of 1.39 $L \cdot min^{-1}$ in both cases. The T1 test was carried out in a commercial 'Big Top' peach orchard (*Prunus persica (L.)* Batsch) with trees trained in an open vase system and located in the IRTA Experimental Station in Gimenells (Lleida, Spain) (latitude: 282807.00 E, longitude: 4614876.00 N).

In the second test (T2), an axial fan air-blast sprayer (Twister 2000, Mañez and Lozano S.L., Valencia, Spain) was used, with a measured air flow rate of 29.700 $m^3 \cdot h^{-1}$ and equipped with 20 operating nozzles. In this case, the nozzles used were ATR 80 Grey (STN-G1) at 1.5 MPa and TVI 8003 Blue (DRN-B1) at 1.3 MPa, operating with flow rates of 2.51 and 2.50 $L \cdot min^{-1}$, respectively. In this case, the test was performed in globular-trained citrus trees, in a commercial 'Clementine' citrus orchard (*Citrus clementine*) located in Roquetes (Tarragona, Spain) (latitude: 286047.00 E, longitude: 4517792.00 N).

In the third and fourth tests (T3 and T4), the sprayer was a conventional axial fan air-blast with deflectors in the upper and bottom part of the arc of the nozzles (Eolo 2091, Teyme Tecnología Agrícola S.L., Torre-Serona, Spain). In test T3, the 10 available nozzles of the sprayer were used and the air flow rate was 55,000 $m^3 \cdot h^{-1}$, while in test T4 only 8 nozzles were used and the

air flow rate was set at 46,200 $m^3 \cdot h^{-1}$. In test T3, the nozzles that were compared were the standard hollow-cone nozzle ATR 80 Grey at 1.0 MPa (STN-G2) and the spray drift reduction hollow-cone nozzle TVI 8003 Blue at 1.0 MPa (DRN-B2), with flow rates of 2.08 and 2.19 $L \cdot min^{-1}$, respectively. In the T4 test, the same ATR 80 Grey (STN-G3) and TVI 8003 Blue (DRN-B3) nozzles were used, although the working pressure in this case was 0.7 MPa for both, and their respective flow rates were 1.76 and 1.83 $L \cdot min^{-1}$.

The T3 test was performed with hedgerow-trained 'Golden' apple trees (*Malus domestica*) in an orchard located in the IRTA Experimental Station at Gimenells (Lleida, Spain) (latitude: 282765.00 E, longitude: 4615309.00 N). The commercial plot where the T4 test was carried out corresponded to a 'Chardonnay' vineyard (*Vitis vinífera*) which employed a trellis training system, located in Raimat (Lleida, Spain) (latitude: 289105.00 E, longitude: 4616616.39 N).

In the fifth test (T5), an air-assisted orchard sprayer (VariMAS 1, Munckhof Fruit Tech Innovators, A.J. Horst, The Netherlands) with an air flow rate of 11700 $m^3 \cdot h^{-1}$ and equipped with 16 operating nozzles was used. This sprayer, which is innovative in the area where the tests were carried out, achieves an optimal leaf coverage and a high spray drift reduction. The nozzles used were ATR 80 Yellow at 0.5 MPa (STN-Y) and TVI 80015 Green at 0.5 MPa (DRN-G) with flow rates of 0.73 and 0.77 $L \cdot min^{-1}$, respectively.

For the sixth and seventh tests (T6 and T7), the spraying equipment used was a conventional axial fan air-blast sprayer (model 2000, Tifone, Cassana, Italy) with an air flow rate of 58,000 $m^3 \cdot h^{-1}$ and equipped with 16 operating nozzles. Two pairs of STN and DRN nozzles were compared using this equipment. In the T6 test, ATR 80 Yellow at 1.6 MPa (STN-Y2) and TVI 80015 Green at 1.4 MPa (DRN-G2) nozzles were used, with flow rates of 1.29 $L \cdot min^{-1}$ and 1.30 $L \cdot min^{-1}$, respectively. In the T7 test, ATR 80 Grey at 0.5 MPa (STN-G4) and TVI 8003 Blue also at 0.5 MPa (DRN-B4) nozzles were used, with flow rates of 1.50 and 1.55 $L \cdot min^{-1}$, respectively.

187 The T5, T6 and T7 tests were conducted in a commercial 'Conference' pear orchard (*Pyrus*
188 *communis*) with a hedgerow training system, located in the IRTA Experimental Station in
189 Mollerussa (Lleida, Spain) (latitude: 322596.05 E, longitude: 4609495.68 N).

190 Table 1 shows the leaf wall area (LWA) and the leaf area index (LAI) values for the testing
191 orchards. The LWA was calculated taking into account the canopy height and the tree spacing
192 between rows, and the LAI, expressed as leaf area per individual tree ground surface area, was
193 calculated for each crop using the method developed by Sanz et al. (2018).

194 **Table 1.** Characteristics of the orchards where the tests were carried out.

Parameters		**3D crops**				
		Peach trees	**Citrus trees**	**Apple trees**	**Vineyard**	**Pear trees**
Test		T1	T2	T3	T4	T5, T6, T7
Orchard	**Cultivar**	Big Top	Clementine	Golden	Chardonnay	Conference
	Area (ha)	0.64	6.67	1.64	0.52	0.73
	Row direction	E-W (-35º)	E-W (18º)	E-W (-70º)	E-W (-83º)	E-W (-115º)
	Training system	Open vase	Globular	Hedgerow	Trellis	Hedgerow
	Tree spacing (between rows x between trees) (m x m)	5.00 x 2.00	6.00 x 4.00	3.45 x 0.60	3.00 x 1.80	3.30 x 1.00
Canopy	**Height, h (m)**	2.90	2.85	2.80	1.25	3.0
	Width along row (m)	2.70[a]	2.80[a]	1.20[b]	2.0[b]	2.0[b]
	Width crossing row (m)	2.95	2.50	1.90	0.86	0.5
	Growth stage (BBCH)	91 (Fruit growth, 60%)	89 (Fruit growth, 95%)	93 (Beginning of leaf fall)	91 (Post-harvest)	74 (Fruit growth, 40%)
	LWA ($m^2 \cdot ha^{-1}$)	11600	9500	16231	8333	18181
	LAI	3.02	3.15	1.80	1.05	2.2

195 a*: Individual trees.*
196 *b: trees growing into each other in the row.*

197 **Table 2.** Description of the spray drift tests.

Test	Date	Crop	Spray drift assessment method	Sprayer	Nozzle		Pressure (MPa)	Nominal flow rate ($L \cdot min^{-1}$)	Forward speed ($km \cdot h^{-1}$)	Operating nozzles	Spray volume ($L \cdot ha^{-1}$)	Air flow rate ($m^3 \cdot h^{-1}$)	Number of replications
					Model	Type							
T1	09/16/2011	Peach	ISO 22866:2005	Hardi Arrow F 1000	ATR 80 Orange	STN-O	1.0	1.39	4.0	20	834	65000	1
					TVI 8002 Yellow	DRN-Y	0.9	1.39					
T2	12/12/2013	Citrus		Mañez & Lozano Twister 2000	ATR 80 Grey	STN-G1	1.5	2.51	1.0	20	2450	29700	5
					TVI 8003 Blue	DRN-B1	1.3	2.50			2500		
T3	11/07/2014	Apple		Teyme EOLO 2091	ATR 80 Grey	STN-G2	1.0	2.08	4.5	10	810	55000	3
					TVI 8003 Blue	DRN-B2	1.0	2.19			860		
T4	10/06/2015	Grape		Teyme EOLO 2091	ATR 80 Grey	STN-G3	0.7	1.76	6.0	8	476	46200	3
					TVI 8003 Blue	DRN-B3	0.7	1.83			487		
T5	06/18/2019	Pear	LiDAR system	Munckhof VariMAS 1	ATR 80 Yellow	STN-Y1	0.5	0.73	5.0	16	427	≃ 12000	5
					TVI 80015 Green	DRN-G1	0.5	0.77			376		
T6	06/19/2019			Tifone 2000	ATR 80 Yellow	STN-Y2	1.6	1.29	5.0	16	755	58000	5
					TVI 80015 Green	DRN-G2	1.4	1.30			761		
T7					ATR 80 Grey	STN-G4	0.5	1.50			878		
					TVI 8003 Blue	DRN-B4	0.5	1.55			907		

198 *STN: Hollow-cone standard nozzle; DRN: Hollow-cone spray drift reduction nozzle.*

199 *2.2. Meteorological conditions*

200 During the development of each test detailed in Section 2.1, the meteorological conditions
201 corresponding to temperature, relative humidity, wind speed and direction were recorded with
202 an acquisition frequency of 1 Hz. In the T1 test, a combined temperature and relative humidity
203 sensor (HMP45 C and Pt 100, Vaisala Inc, Vaanta, Finland), and a wind speed and direction
204 sensor (05103, RM Young, Traverse City, MI, USA) were used. All sensors were connected to
205 a datalogger (CR510, Campbell Scientific Inc, Logan, UT, USA). In contrast, in tests T2, T3
206 and T4, a portable weather station equipped with temperature (model MCP9808, Adafruit
207 Industries LLC, New York, NY, USA), humidity (model HIH 5030/5031, Honeywell, Golden
208 Valley, MN, USA), wind speed (model Watson 8681-WSS, W&S, Hockley, Essex, UK), and
209 wind direction (ACE-128 encoder, Bourns, Riverside, CA, USA) sensors were used. Finally, in
210 tests T5, T6 and T7, the weather conditions were recorded using a compact ultrasonic weather
211 station (WXH220 model, Airmar Technology Corporation, Milford, NH, USA).

212 In tests T1-T4, all sensors were placed on a mast located 20 m away from the last row of trees.
213 The temperature and relative humidity sensors were installed at 4 m high and the wind speed
214 and direction sensors at 7 m high. In tests T5-T7, the weather station was located at the
215 beginning of the last row of trees, at a height of 7 m.

216 Table 3 shows the recorded meteorological data, indicating the average values for each of the
217 tests. These measurements comply with the ranges established in ISO 22866:2005: wind speed
218 between 1 and 3 $m \cdot s^{-1}$ with no more than 10% of wind measurements lower than 1 $m \cdot s^{1}$, and
219 wind direction in the range of ± 30º to the perpendicular to the spray track with no more than
220 30% of results upper 45º.

221 **Table 3.** Meteorological conditions during the tests. The average values of temperature, relative humidity, wind
222 speed and wind direction are shown.

Test	Nozzle	T (ºC)	RH (%)	Wind speed ($m \cdot s^{-1}$)	Wind direction[1] (º)	Wind speed measurements <1 $m \cdot s^{-1}$ (%)	Wind direction measurements upper ±45º (%)
T1	STN-O	20.7	57.8	1.2	8.3	8.2	6.5
	DRN-Y	21.3	57.0	1.4	6.9	7.6	4.1
T2	STN-G1	9.1	61.3	2.2	-20.8		1.9
	DRN-B1	9.4	61.2	1.9	-20.4		5.4
T3	STN-G2	16.4	53.5	1.8	-14.2		3.7
	DRN-B2	15.3	50.0	1.6	-9.4		2.5
T4	STN-G3	20.5	48.9	2.2	-5.3		9.6
	DRN-B3	21.2	48.2	2.6	-3.8		7.4
T5	STN-Y	23.2	31.0	2.5	-15.1	0.0	15.8
	DRN-G	23.9	30.6	2.9	-13.6		12.1
T6	STN-Y	21.3	41.1	2.2	16.3		17.3
	DRN-G	23.1	40.6	2.5	13.9		15.2
T7	STN-G4	23.7	35.6	1.7	22.7		19.1
	DRN-B4	24.4	35.1	2.2	19.4		17.8

223 [1] *Wind direction respect to the perpendicular of tree rows.*

224 *2.3. ISO 22866:2005 methodology*

225 In the T1, T2, T3 and T4 tests, detailed in Table 1, the ISO 22866:2005 based methodology was
226 applied. Prior to the performance of all tests, the equipment was calibrated by adjusting the
227 application volume to the tree structure and the foliar density of the canopy. To evaluate the
228 airborne spray drift, 6 m long nylon string collectors were fixed vertically to two masts
229 positioned, respectively, at 5 m and 10 m from the center of the last alley of the plot and
230 perpendicular to it. Two collectors spaced 2 m apart were placed on each of the masts. To
231 evaluate the sedimenting spray drift, terrestrial collectors were used, in this case 0.515x0.065 m
232 horizontal blotting paper collectors (73 $g \cdot m^{-2}$ filters, Anoia S.A., Barcelona, Spain). These were
233 distributed in 3 columns separated 1.5 m from the center of each collector and positioned at the
234 following perpendicular distances from the center of the last alley of the plot: 1.5, 2.5, 5. 7.5,
235 10, 12.5, 15, 17.5, 20, 25, 30, 35 and 40 m. The sprayed liquid was a mixture of tap water and
236 brilliant sulfoflavine (BSF) tracer at 1 $g \cdot L^{-1}$. In order to know the concentration of the mixture
237 in the tank, two samples were taken from a spray nozzle, one before application and the other
238 after. In Torrent et al. (2017), a detailed description of the methodology applied is presented.

239 In test T1, carried out in peach trees, the STN-O and DRN-Y nozzles were contrasted,
240 performing one repetition for each nozzle type. The forward speed was 4 $km \cdot h^{-1}$, applying a
241 volume of 834 $L \cdot ha^{-1}$. The treatment area included a total of 4 alleys (3 alleys where both sides
242 were sprayed and 2 half-alleys where spraying was only performed on the side of the
243 vegetation), so the treated width was 20 m.

244 The T2 test was performed in citrus using the STN-G1 and DRN-B1 nozzles, with a total of 5
245 repetitions for each nozzle type. The forward speed was 1.0 $km \cdot h^{-1}$, applying a volume of 2450
246 $L \cdot ha^{-1}$ with the STN-G1 and 2500 $L \cdot ha^{-1}$ with the DRN-B1. The treated area also consisted of 4
247 alleys, being the treated width of 24 m.

248 In the T3 test, conducted on apple trees, the application was carried out with the STN-G2 and
249 DRN-B2 nozzles, with a total of 3 repetitions for both nozzle types. The forward speed was 4.5

km·h^{-1} and the application volume was 810 L·ha^{-1} for the STN-G2 nozzles and 860 L·ha^{-1} for the DRN-B2 nozzles. The treated width was 24 m, corresponding to 7 alleys.

Finally, in the T4 test conducted in a vineyard, the nozzles used were the STN-G3 and the DRN-B3, with 3 repetitions in both cases. The forward speed was 6.0 km·h^{-1}, and the applied volume 476 L·ha^{-1} for the STN-G3 and 487 L·ha^{-1} for the DRN-B3. In this case, the treated area consisted of 7 alleys with a treated width of 21 m.

The arrangement of the vertical masts for the detection of aerial spray drift in the four plots on which spray drift was evaluated is shown in Fig. 1.

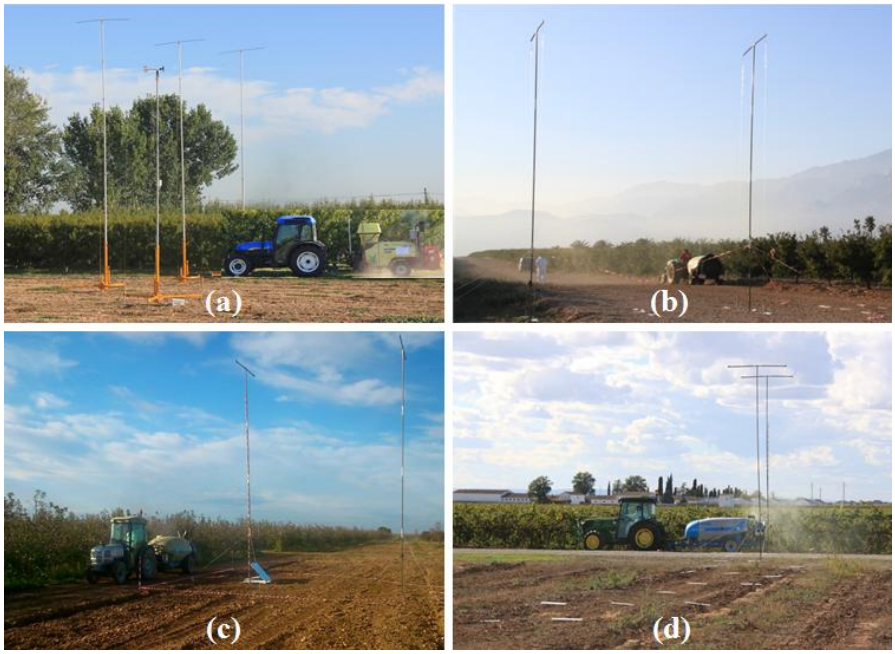

Fig. 1. Orchards tested for spray drift assessment with vertical and horizontal collectors: a) peach trees; b) citrus; c) apple trees; d) vineyard.

2.4. LiDAR methodology

In tests T5, T6 and T7, spray drift under field conditions was evaluated using an ad hoc LiDAR system developed by Gregorio et al. (2015, 2016). This instrument has a laser emitter (Er-glass laser) with a wavelength of 1534 nm, which emits pulses of 3 mJ energy and 6 ns duration. The backscattered light is captured by a telescope with 80 mm aperture, and, through a set of optics,

267 is focused on the photodetector surface of an avalanche photodiode (APD) module that converts
268 the light signal received into an electrical signal. As shown in Fig. 2, the emission and receiving
269 subsystems have a pan & tilt unit, which allows azimuth and elevation scanning. This LiDAR
270 system is eye safe and has a spatial resolution of 2.4 m.

271 The tests T5, T6 and T7 were carried out in pear trees, performing the treatment only along the
272 second path, spraying at both sides, with a forward speed of 5 km·h^{-1}. In the T5 test, the STN-
273 Y1 (427 L·ha^{-1}) and DRN-G1 (376 L·ha^{-1}) nozzles were compared; in the T6 test, the STN-Y2
274 (755 L·ha^{-1}) and the DRN-G2 (761 L·ha^{-1}); and in the T7 test, the nozzles compared were the
275 STN-G4 (878 L·ha^{-1}) and DRN-B4 (907 L·ha^{-1}). A total of 5 repetitions were carried out with
276 each of the aforementioned nozzles.

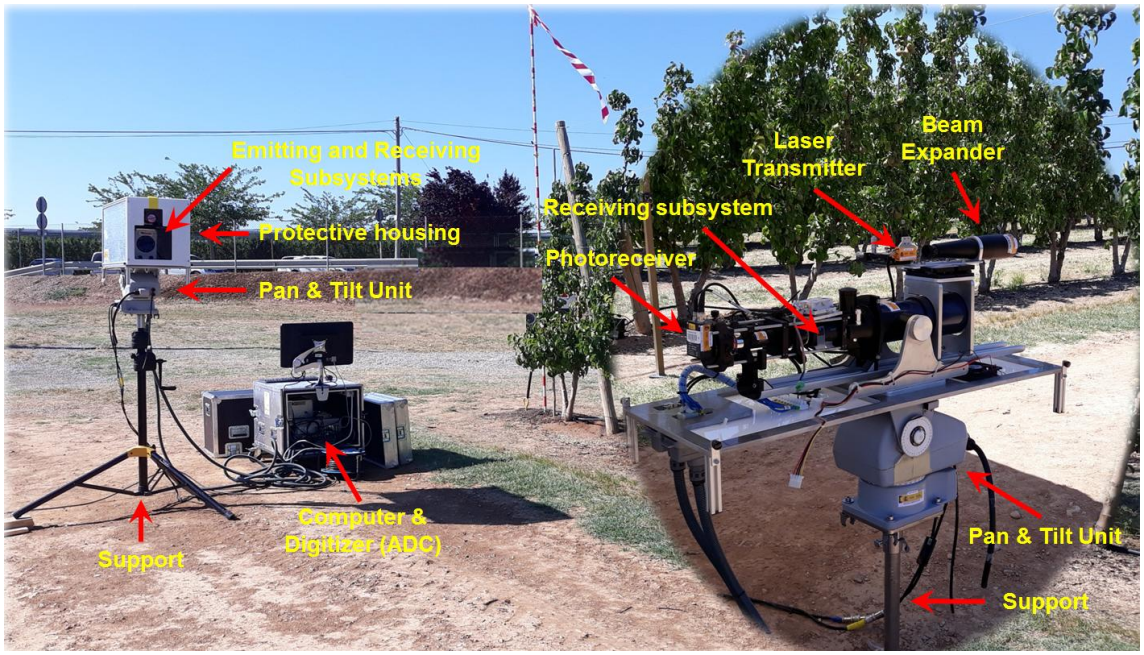

277

278 **Fig. 2.** (Left) LiDAR system used for the spray drift assessment in tests T5, T6 and T7; (Right) zoom view of the
279 emission and receiving subsystems (without the protective housing) where internal optoelectronic components are
280 shown.

281 As shown in Fig. 3a, the LiDAR system was placed parallel to the last row of trees at a distance
282 of 3.3 m from it, equivalent to the width of one of the alleys of that plot. The height of the
283 emitter and receiver system with respect to the ground was 0.8 m. This height was determined
284 to avoid the ground irregularities and the impact of the laser beam to the ground.

In Fig. 3b the type of measurement is presented, consisting of scans in the vertical plane, with a scanning angle of 4.5º. This angle was set so that the scan collected the entire spray drift cloud, starting at a minimum height of 3.9 m and a vertical resolution of 1.0 m at the beginning of the treatment area, until reaching 7.2 m in height and a vertical resolution of 1.8 m at the end of this area. The angular velocity was 1.13°/s and the pulse rate frequency 1 Hz. The objective with this methodology was to evaluate the spray drift cloud that passed through a window parallel to the last row of trees. In this way, parameters such as sweep angle, angular velocity and pulse rate frequency allow adjustment of the spatial and temporal resolution of LiDAR measurements.

Spraying started at 50 m from the LiDAR system and ended at 92 m, so the sprayed length was 42 m. The following measurement sequence was followed: Start of the LiDAR measurement (laser emission) (T=0s); Spray start (T=30 s); End of spraying and stopping the tractor (T=60 s); End of the LiDAR measurement (T=100 s).

During the first 30 s (before starting the spraying), measurements of the background signal, necessary for post-processing, were made. In addition, it should be noted that, before each spray drift test, tests were performed for the presence of dust generated by the motion of the tractor-sprayer equipment and by the fan itself. If dust was detected, the ground was wetted to avoid significant distortion of the background signal.

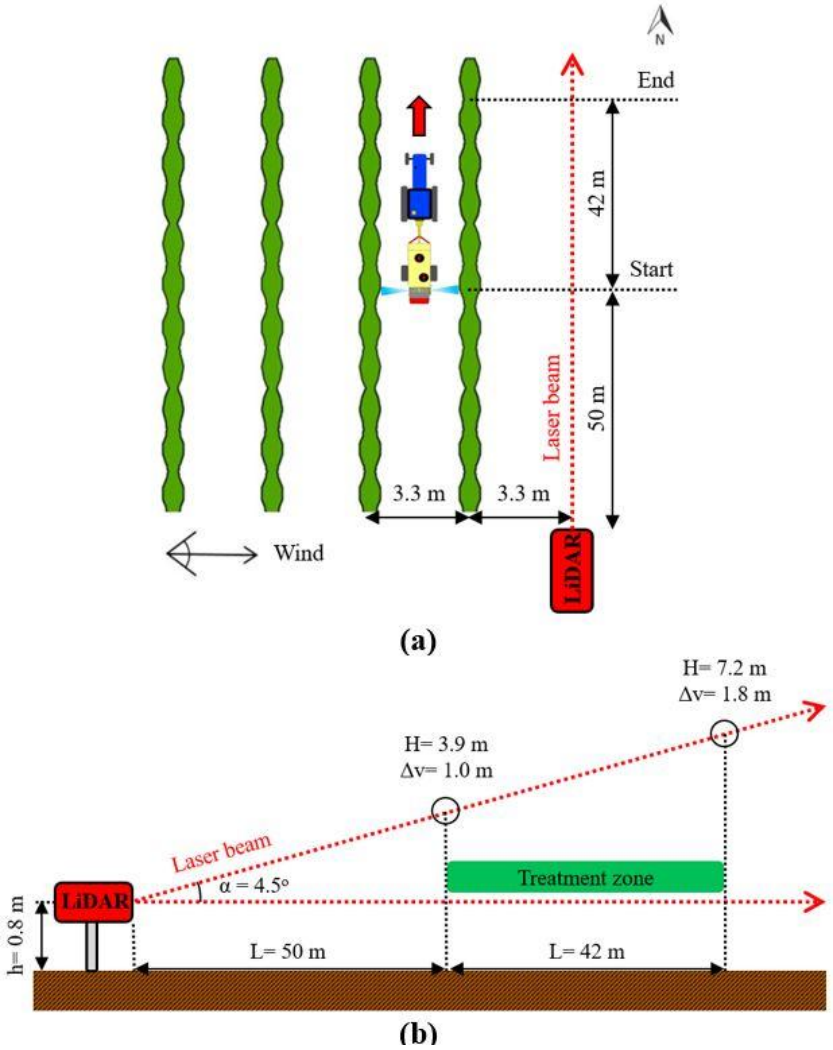

Fig. 3. Schematic representation of the LiDAR scan performed during tests T5, T6 and T7: a) plan view; b) side view. L: Length, H: Height, Δv_i: Vertical resolution of LiDAR measurements considering a pulse repetition rate of 1 Hz.

2.5. Data analysis

2.5.1. ISO spray drift tests

2.5.1.1. Experimental design analysis

Two linear models were formulated for each of the crops tested as proposed by Garcerá et al. (2017) in similar PPP studies. In the first model (airborne spray drift deposition), an analysis of variance (ANOVA) for a three-way factorial treatment structure was adopted. The analysis of vertical deposits (dependent variable in the model) allowed significant effects of fixed factors such as nozzle type (α), distance to the tree row (β), and collector height (γ) to be assessed.

315 Other factors such as crop type, air assistance capacity and wind speed were only considered at
316 qualitative level. So, the proposed model was as follows,

317 $$y_{ijkl} = \mu + \alpha_i + \beta_j + \gamma_k + \alpha\beta_{ij} + \alpha\gamma_{ik} + \beta\gamma_{jk} + \alpha\beta\gamma_{ijk} + e_{ijkl} \quad (1)$$

318 where i = 1, 2; j = 1, 2; k = 1…6, with y_{ijkl} the vertical deposit value l obtained at height k (1, 2,
319 3, 4, 5 or 6 m) and distance j (5 or 10 m) for nozzle i (STN or DRN); μ is the general average;
320 α_i the effect of level i of the fixed factor A (nozzle type); β_j the effect of level j of the fixed
321 factor B (distance); γ_k the effect of level k of the fixed factor C (collector height);
322 $\alpha\beta_{ij}; \alpha\gamma_{ik}; \beta\gamma_{jk}; \alpha\beta\gamma_{ijk}$ the effects of the interactions between fixed factors A, B and C; and
323 e_{ijkl} is the error term.

324 The second model was simpler. Considering now the sedimenting spray drift deposition as
325 dependent variable, significant effects of nozzle type and distance of spray drift detection were
326 tested through a two-way factorial fixed model formulated as before, according to the following
327 expression:

328 $$y_{ijl} = \mu + \alpha_i + \beta_j + \alpha\beta_{ij} + e_{ijl} \quad (2)$$

329 where i = 1, 2; j = 1…13, with y_{ijl} the horizontal deposit value l obtained at distance j (1.5, 2.5,
330 5, 7.5, 10, 12.5, 15, 17.5, 20, 25, 30, 35 or 40 m) for nozzle i (STN or DRN); μ is the general
331 average; α_i the effect of level i of the fixed factor A (nozzle type); β_j the effect of level j of the
332 fixed factor B (detection horizontal distance); $\alpha\beta_{ij}$ the effect of the interaction between the fixed
333 factors A and B; and e_{ijl} the error term.

334 In both factorial analyses, Box-Cox transformations were applied to the data when necessary to
335 meet the assumptions of homogeneity of variance (Bartlett test) and normality (Shapiro-Wilk
336 test). The Tukey honest significant difference (HSD) test was used in each case as a pairwise
337 multiple comparisons technique to search for specific differences. In all tests, a confidence level
338 of 95% was considered. Open source RStudio software (version 1.2.1335) was used for data
339 analysis.

2.5.1.2. Spray drift potential reduction

The spray drift recovery obtained in each ISO test was calculated according to the following expressions:

$$CR_V = \sum_{k=1}^{6} V_{F(k)} \quad (3)$$

$$CR_H = \sum_{j=1}^{13} V_{F(j)} \quad (4)$$

where CR_V and CR_H are the total airborne spray drift recovery (%) and the total sedimenting spray drift recovery (%), respectively; and $V_{F(k)}$ and $V_{F(j)}$ are the airborne spray drift at the vertical section of the collector line k (%) and the sedimenting spray drift at the horizontal collector j (%), respectively. Airborne spray drift was computed on the basis of the spray drift deposits to the corresponding sections of the collectors, following the procedure detailed in Torrent et al. (2017).

In each of the tests, the calculation of the spray drift potential reduction (DPR) was made from the spray drift recovery values of the candidate nozzle and the reference nozzle, applying the following expression:

$$DPR = \left(1 - (CR_C / CR_R)\right) \cdot 100 \quad (5)$$

where CR_C is the spray drift potential of the candidate nozzle (%) and CR_R is the spray drift potential of the reference nozzle (%).

2.5.1.3. Regression functions for sedimenting spray drift

A total of eight continuous functions of the variable sedimenting spray drift were determined as a function of distance, corresponding to the combination of each type of crop (peach, citrus, apple and grape) and nozzle (STN and DRN). For this, the regression functions were found

362 from the mean values of the set of repetitions (tests T1, T2, T3 and T4). The regression function
363 that presented a better fit in all cases was exponential, according to the following expression:

364 $$y = a * Exp^{(-b \cdot x)} \quad (6)$$

365 where *y* represents the deposition of the sedimenting spray drift (%); *a* the scale factor; *b* the
366 growth rate; and *x* the distance (m).

367 Two additional regression functions were obtained for each kind of nozzle considering the set of
368 depositions obtained in all crops, with the exception of apple, since its growth stage (leaf fall)
369 was different from the rest of the crops. For all functions, the values corresponding to the root
370 mean square error (RMSE) and the coefficient of determination (R^2) were obtained. Also,
371 constant variance and autocorrelation diagnosis were checked on the linearized model to meet
372 the corresponding assumptions. Finally, from the regression functions obtained, the buffer zones
373 corresponding to the 10%, 5% and 1% spray drift values were determined based on the total
374 collected, for each crop and nozzle type (STN and DRN).

375

376 *2.5.2. LiDAR spray drift tests*

377 Post-processing of the data obtained with the LiDAR system was carried out through the
378 numerical computing software Matlab (R2018a, MathWorks Inc., Nastik, Massachusetts, USA).
379 The resulting LiDAR signal was background and range-corrected. To determine the background
380 signal, the measurements taken during the first 30 s of each scan sequence were considered. The
381 range correction took into account that the LiDAR signal decreases with the square of the
382 distance (Wandinger, 2005). From the corrected signal, the integrated LiDAR signal (S_{Int}),
383 normalized by the sprayed volume and by the laser pulse repetition rate, was calculated
384 following the procedure described by Gregorio et al. (2019). The calculation of the reduction
385 potential of the nozzles using the LiDAR (DPR_{lidar}) system was performed according to the
386 following expression:

$$DPR_{lidar} = \left(1 - \frac{S_{Int,C}}{S_{Int,R}}\right) \cdot 100 \quad (7)$$

where $S_{Int,C}$ and $S_{Int,R}$ are the integrated LiDAR signal of the candidate nozzle and the reference nozzle, respectively.

As in the case of the ISO tests, an ANOVA for a particular sprayer (Tifone) was carried out based on the data of the integrated LiDAR signal, with the aim of assessing the effect of nozzle type. In this case, it was necessary to perform a signal transformation (inverse function) to meet the assumptions of data normality and homoscedasticity. Subsequently, a two-way ANOVA was conducted to assess the effect of nozzle (STN and DRN) and sprayer (Tifone and Munckhof) on the spray drift detected by the LiDAR system. To meet the assumptions in this case, square root transformation of the LiDAR signal was necessary.

3. Results

3.1. Spray drift assessment based on ISO methodology

The average values of the airborne spray drift measured at distances of 5 and 10 m, up to a height of 6 m, for the four crops (tests T1, T2, T3 and T4) and the two types of nozzle (STN and DRN) tested, are represented in the bar graphs of Fig. 4 with their respective standard error. The deposits of spray drift values at 6 m were higher than the acceptable level specified in the ISO 22866:2005, because the deposits on this height related to the total spray drift collected were greater than the 10%. On the other hand, the high deposits around or upper the 100% were probably due to the air turbulences, so some droplets were deposited on both sides and on the back part of vertical collectors. In the statistical analysis, the significance of the main effects (nozzle type, height and distance) and the existence of any interaction between them were studied. The results showed significant differences between the nozzle type in all crops. In contrast, the height effect was only significant for peach trees (specifically at the height of 1 m)

411 and apple trees (height of 6 m). With respect to the distance effect, this was significant for all
412 crops and nozzle types except for DRN in peach trees.

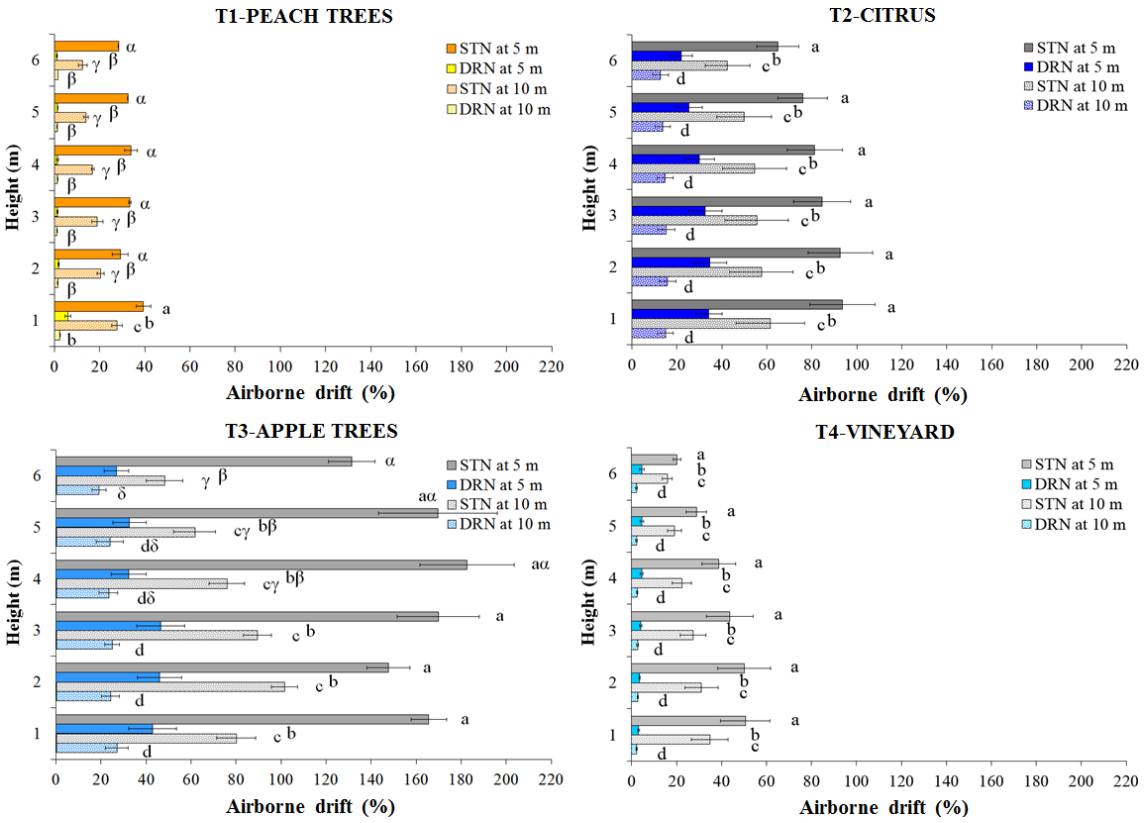

413

414 **Fig. 4.** Airborne spray drift (mean value and standard error) and variance analysis (tests T1, T2, T3 and T4). Four
415 orchards (peach trees, citrus, apple trees and vineyard), two nozzle types (STN and DRN), two distances (5 m and 10
416 m), and six heights (1-6 m) were tested.
417

418 In Fig. 5, the mean sedimenting spray drift values are shown for each sampled distance between
419 1.5 and 40 m (between 2.5 and 40 m for peach trees), for the two types of nozzle and the four
420 crops considered in this work. Being significant the interaction nozzle-distance, Fig. 5 shows
421 the spray drift deposit variation for both nozzles (STN and DRN) as we move away from the
422 source of drift. With the exception of peach trees, differences between nozzles were only
423 significant for certain distances, in general, for those closest to the source of the drift. In the case
424 of peach trees, there are significant differences between the two nozzle types (STN and DRN) at
425 all distances, with the STN values higher than those of the DRN, except at the distance of 2.5 m.
426 For the rest of the crops, significant differences were found at the following distances: citrus

427 (7.5-25 m and 40 m), apple trees (2.5-15 m) and vineyard (7.5-30 m). For both nozzle types and
428 in all crops, a clear decreasing trend in sedimenting spray drift is observed as the distance
429 increases up to 15 m. Above this distance, it can be seen how spray drift reduction is practically
430 negligible since it takes very low values. The higher sedimenting spray drift values in the first
431 7.5 m in the case of apple trees compared to other crops should also be noted.

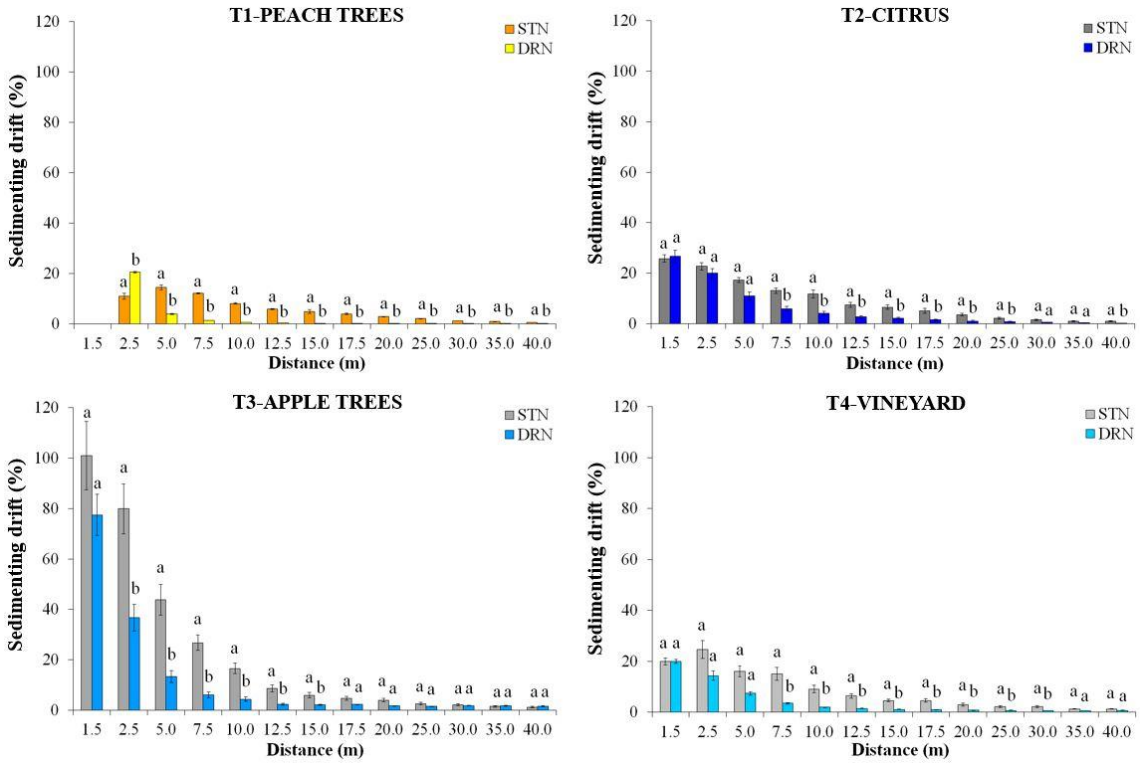

432

433 **Fig. 5.** Sedimenting spray drift (mean value and standard error) and variance analysis (tests T1, T2, T3 and T4). Four
434 orchards (peach trees, citrus, apple trees and vineyard), two nozzle types (STN and DRN), and thirteen distances (1.5-
435 40 m) were tested.

436

437 The exponential functions fitted from the sedimenting spray drift values in each of the tests and
438 for both nozzle types are presented in Fig. 6. In all cases a good fit is observed, with R^2 values
439 above 0.7. Another aspect to highlight is that the functions that estimate the deposition of the
440 DRN have a scale factor (a) greater than that of the STN, as well as a decrease rate (b) between
441 two and eight times higher. The highest rate of decline corresponded to peach trees for the DRN
442 nozzle type, followed by the apple trees-DRN, vineyard-DRN and citrus-DRN combinations.

443 Generic sedimenting spray drift curves for both nozzle types (STN and DRN) were also
444 generated from the measurements obtained in three of the four crops (peach, citrus and grape).
445 This was due to the major difference between the sedimenting spray drift values obtained in
446 apple compared to the other crops.

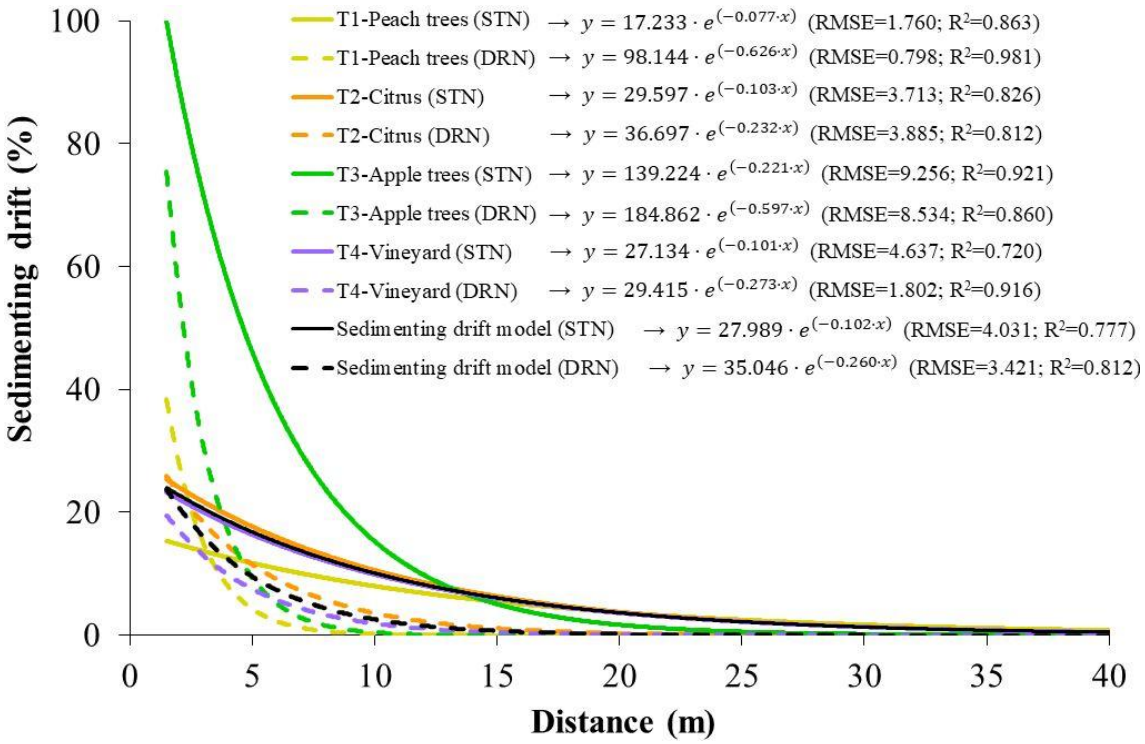

447

448 **Fig. 6.** Fitted exponential functions of the sedimenting spray drift for the different tested orchards and nozzle types.

449

450 The buffer zones were determined on the basis of the fitted exponential functions. These were
451 found by establishing, for each nozzle in each crop, the following maximum percentages of
452 sedimenting spray drift that are allowed outside the treatment area: 10%, 5% and 1%. As can be
453 seen in Fig. 7, the distances of the buffer zones for the DRN are reduced by about 50% in
454 relation to the STN for citrus, apple trees and vineyard. In the case of peach trees, the reduction
455 of the buffer zone achieved by the DRN was greater than 75%. Equivalently, the buffer zone
456 distances are also presented in terms of the number of rows that should be left untreated to
457 prevent spray drift from reaching non-target areas (see values in brackets in Fig. 7), without
458 considering the filtering capacity of the outside tree rows which could contribute to reduce the

spray drift. The crops in which the longest buffer zones were obtained were peach when SNTs are used and citrus when species are compared using DRN.

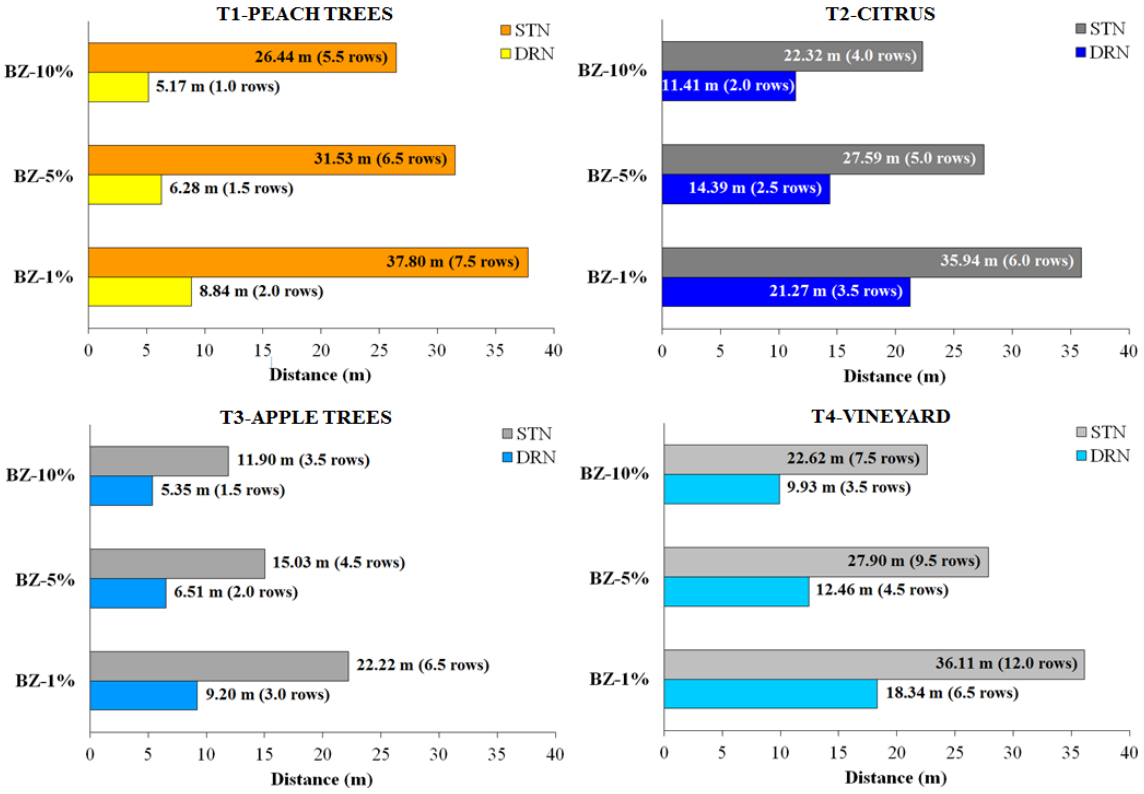

Fig. 7. Buffer zones corresponding to different percentages of sedimenting spray drift allowed outside the treated zone (10%, 5% and 1%). The equivalent distance in rows without treatment is shown in brackets.

Table 4 shows the DPR values of the DRN nozzles compared to the STN, corresponding to airborne spray drift at 5 m and 10 m ($DPR_{V(5m)}$ and $DPR_{V(10m)}$) and sedimenting spray drift (DPR_H). The greatest spray drift reductions were obtained with the DRN nozzles in the T1 test (peach trees), followed by the T4 test (vineyard), the T3 test (apple trees) and the T2 test (citrus), with the exception of the DPR_H of the T4 test which was slightly lower than that of the T3 test. The values of $DPR_{V(5m)}$ and $DPR_{V(10m)}$ were similar in all the tests performed. On the other hand, the DPR_H values were lower than those for DPR_V in all the crops evaluated.

Table 4. DPR values (%) for STN and DRN nozzle type comparisons (tests T1, T2, T3 and T4).

Test	Nozzle	$CR_{V(5\ m)}$ (%)	$CR_{V(10\ m)}$ (%)	CR_H (%)	$DPR_{V(5m)}$ (%)	$DPR_{V(10m)}$ (%)	DPR_H (%)
T1	STN-O	6.96	3.70	13.27	-	-	-
	DRN-Y	0.39	0.33	4.08	94.42	91.20	69.28
T2	STN-G1	24.12	15.78	12.66	-	-	-
	DRN-B1	8.73	4.60	7.63	63.82	70.84	39.75
T3	STN-G2	22.16	10.23	24.07	-	-	-
	DRN-B2	5.18	2.93	8.85	76.61	71.38	63.26
T4	STN-G3	10.57	7.01	11.09	-	-	-
	DRN-B3	1.17	0.70	4.52	88.95	90.00	59.27

3.2. Spray drift assessment based on LiDAR measurements

The results corresponding to the T5, T6 and T7 tests, in which the spray drift was evaluated using a LiDAR system, are presented below. Fig. 8 shows the range profile of the LiDAR signal corresponding to two different sprayers (Munckhof VariMAS 1 and Tifone 2000), with two nozzle types (STN and DRN). As expected, the DRN presented much lower signal values compared to the STN. The configurations that presented the highest signal values were the STN (Y2 and G4) with the Tifone sprayer, while the Munckhof configuration with the DRN-G1 generated the lowest.

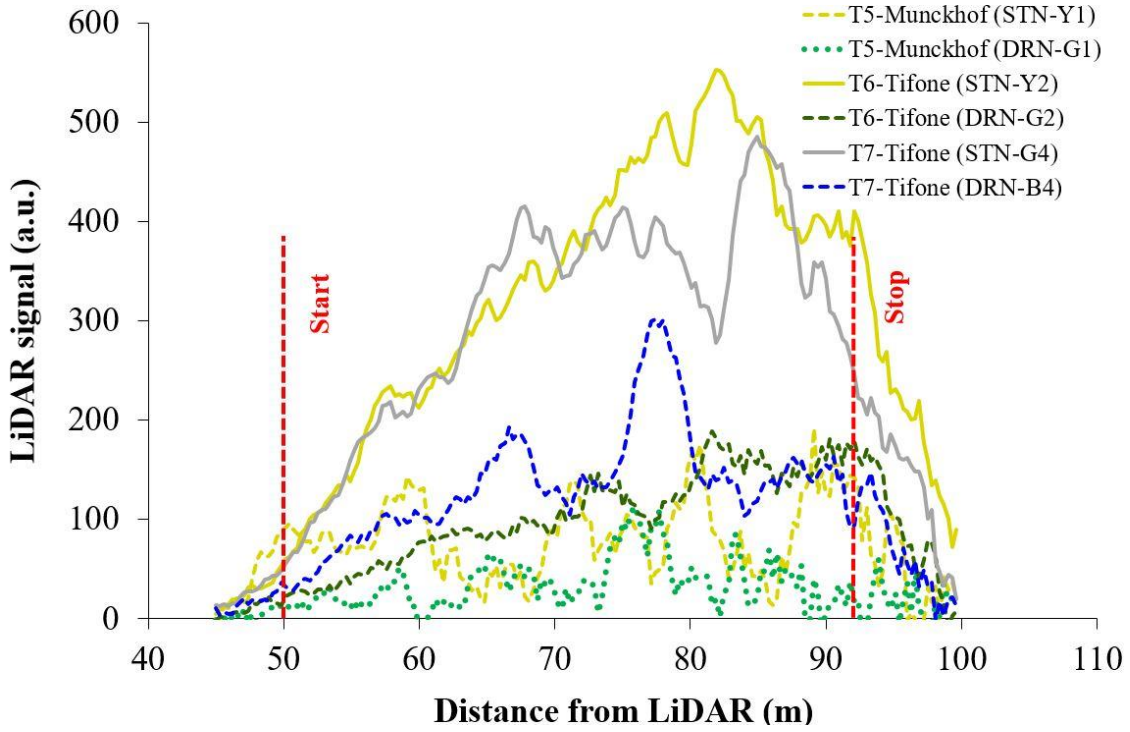

Fig. 8. Nozzle type comparison (STN vs. DRN) based on range profile of LiDAR returns. The LiDAR signal was normalized by the total sprayed volume.

Table 5 shows the DPR values obtained from the integrated LiDAR signals (S_{Int}). It is observed that, regardless of the sprayer used, all DRN reduction values are more than 50% compared to the respective STN values. It is also observed that, when comparing the ATR 80 Yellow and TVI 80015 Green nozzles, the DPR values are similar for both sprayers.

In addition, a statistical analysis was carried out based on the S_{Int} values to determine the effect of nozzle and sprayer. The results showed significant differences between the nozzles tested (STN and DRN) in both sprayers, with the DRN obtaining the smallest signal. There were also significant differences between sprayers, with the highest LiDAR signals obtained for the Tifone sprayer regardless of nozzle type.

496 **Table 5.** LiDAR-based DPR values (%) for nozzle and sprayer type comparison (tests T5, T6 and T7).

Test	Sprayer	Nozzle		Pressure	DPR_{lidar}
		Model	Type	(kPa)	(%)
T5	Munckhof VariMAS 1	ATR 80 Yellow	HC-STN	500	-
		TVI 80015 Green	HC-DRN		70.41
T6	Tifone 2000	ATR 80 Yellow	HC-STN	1600	-
		TVI 80015 Green	HC-DRN	1400	68.46
T7		ATR 80 Grey	HC-STN	500	-
		TVI 8003 Blue	HC-DRN		55.38

497 *HC-STN: Hollow-cone standard nozzle; HC-DRN: Hollow-cone spray drift reduction nozzle.*

498

499 In Fig. 9, DPR values are presented by comparing STN and DRN nozzles (ATR 80 Grey and
500 TVI 8003 Blue at 1.0 MPa) using different methods of evaluation. These values include the
501 results obtained by Torrent et al. (2019) using the PDPA (D_{V50}, V_{100} and V_{200}) and wind tunnel
502 (WT_H and WT_V), with the LiDAR system (Gregorio et al. (2019) under laboratory and field
503 conditions ($S_{L(Lab)}$ and $S_{L(Field)}$) and those corresponding to the T3 test (apple trees) of this work
504 (F_H, $F_{V(5m)}$ and $F_{V(10m)}$). It can be seen how the DPR values obtained with each of the different
505 methods are greater than 50%, with the highest DPR values obtained with the parameters V_{100}
506 (98.97%) and V_{200} (96.38%) and the lowest with $S_{L(Field)}$ (57.20%) and WT_H (58.50%). In
507 addition, a statistical analysis was carried out to study whether there were significant differences
508 between the different methodologies. From the results of this analysis, the parameters studied
509 can be grouped as follows: group A (D_{V50}, WT_V, $F_{V(5m)}$ and $F_{V(10m)}$), group B (V_{100} and V_{200}),
510 group C (WT_H, $S_{L(Field)}$ and F_H) and group D ($S_{L(Lab)}$).

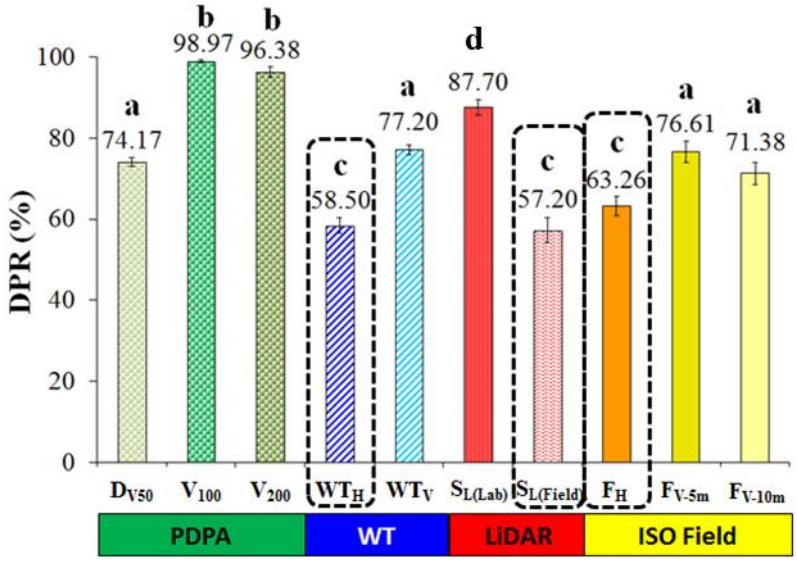

Fig. 9. Indirect and direct methods comparison for the hollow-cone nozzles ATR 80 Grey and TVI 8003 Blue in apple trees application. The DPR values (mean±SE) are shown. Different letters indicate statistically significant differences (Tukey's HSD test, $p<0.05$).

4. Discussion

In the spray drift evaluation tests for the 4 crops studied (peach, citrus, apple and grape), both airborne and sedimenting spray drift were evaluated. In all cases, the airborne spray drift generated by the STN was significantly greater than that generated by the DRN, with the latter showing a clear reduction effect regardless of crop type or distance to the treatment area. In addition, the airborne spray drift evaluated at a distance of 5 m from the treatment area was much greater than at 10 m, as expected. The results confirmed that the type of nozzle used is one of the most influential and effective variable for spray drift control. Also, it should be noted that the airborne drift values were much higher than those for sedimenting spray drift.

With respect to sedimenting spray drift, a clear buffer zone for each nozzle type (STN and DRN) was obtained, with a significant reduction of sedimenting spray drift obtained at close distances (2.5-7.5 m) and remote distances (15-30 m). Nonetheless, most of the sedimenting spray drift was concentrated in the first 10-15 m, distances which should be taken into account when sizing buffer zones to prevent the contamination of nearby water bodies or adjacent crops.

530 The high airborne and sedimenting spray drift values obtained in apple can be attributed to the
531 growth stage (BBCH 93, beginning of leaf fall) of the crop itself at the time the spray drift tests
532 were made and to the high value of the air flow rate. Due to the fall of the leaves, the percentage
533 of gaps was higher than in the rest of the crops, offering less resistance to the passage of the
534 droplets. It is clear then, that crop growth stage is a very important variable in relation to spray
535 drift, and should be taken into account when establishing spray drift models. Indeed, in the
536 biexponential spray drift model established by Holterman et al. (2017), the BBCH growth stage
537 variable was in fact taken into account.

538 The functions that best fitted the sedimenting spray drift data were those of the exponential
539 type. The fitted functions of the DRN presented scale factors and decrease rates higher than
540 those of the STN. This is attributable to the fact that the DRN nozzles had higher sedimenting
541 spray drift at close distances and a higher reduction effect as distance increases. Of the set of
542 crops tested in full leaf stages, special attention should be paid to citrus since, due to their
543 globular shape and the high volumes of spray liquid that are applied to reach all parts of the
544 canopy, more airborne spray drift is generated than with the other crops. In this line, the German
545 model (Ganzelmeier et al., 1995; Rautmann et al., 2001) shows a strong reduction of spray drift
546 in the first 5 meters, as do the spray drift functions presented in this work. Despite this, the
547 German model overestimates the sedimenting spray drift generated for the STN in citrus in the
548 first 2.5 m and, above this distance, underestimates it.

549 Using DRN instead of STN allows over a 50% reduction in the distance of the buffer zones. In
550 this way, production losses due to non-treatment could be avoided as, in small plots, the
551 solution which is proposed is not to treat instead of leaving an uncultivated area. It should also
552 be noted that the functions obtained for apple start from much higher scale factors than the other
553 crops as, in this case, very high deposition values were obtained in the first 7.5 m compared to
554 the other crops (Fig. 5).

With respect to DPR, special note should be made of the high reduction capacity of DRN compared to STN, especially for airborne spray drift. This confirms how nozzle type is one of the best DRTs for practical purposes for any of the 3D crops tested in the southern part of Europe, since it does not require the implementation of any changes to the plot and its cost is very low.

The new methodology developed to evaluate spray drift in real field conditions using the LiDAR system allowed real-time measurement of the spray drift cloud generated during the treatment, with a high spatio-temporal resolution. This was achieved by scanning the spray drift cloud in a vertical plane with the LiDAR system, which is able to differentiate the spray drift produced by different configurations of the spray-nozzle assembly. In addition to facilitating spray drift evaluation logistics and operations, this new methodology can be adapted to any type of plot and has a very short execution time since it does not require a free strip of land adjacent to the plot to perform measurements. In this way, numerous tests can be carried out, substantially reducing the staff, time and space requirements when following the ISO 22866:2005 methodology.

As previously mentioned, one of the main advantages of the LiDAR system is the evaluation of spray drift in real time (Fig. 8), along with its ability to determine the spray drift profile as a function of distance. This allows the detection of fluctuations in spray drift generated during the application, which are mainly due to variations in the percentage of gaps present in the canopy or to weather conditions (wind speed and direction). According to the results of Table 5, for practical treatment purposes (sprayer calibrated according to the crop), the DRN (TVI 80015 Green) presented a similar reduction regardless of the type of machine used (T5: 70.41%; T6: 68.46%); therefore, in this case, the reduction due to sprayer and nozzle type is a cumulative effect. Comparing the DPR results obtained in the T5 and T7 tests for DRN (TVI 80015 Green and TVI 8003 Blue) at the pressure of 500 kPa (Table 5) with their equivalents in the PDPA (DPR_{V100}: 99.34% and 98.54%) and wind tunnel (DPR_H: 88.24% and 58.50%; DPR_V: 86.86% and 77.20%) (Torrent et al., 2019) tests, some similarity can be observed with the wind tunnel

582 (WT) results for sedimenting spray drift, with the latter higher as they were carried out in a
583 confined space and under controlled environmental conditions.

584 In the comparison between the DPR results obtained in the T3 test with the ATR 80 Grey and
585 TVI 8003 Blue nozzles at 1 MPa using the ISO 22866:2005 methodology (F_H=63.26%,
586 $F_{V(5m)}$=76.61% and $F_{V(10m)}$=71.38%) with those obtained with the indirect methods (PDPA and
587 WT) and the LiDAR system, a very good correspondence was obtained between the F_H
588 parameter and the results obtained with the LiDAR system in field conditions ($S_{L(Field)}$=57.20%)
589 and the WT sedimenting spray drift parameter (WT_H=58.50%). In contrast, the values of the
590 $F_{V(5m)}$ and $F_{V(10m)}$ parameters were similar to those obtained with the PDPA (D_{V50}=74.17%) and
591 the WT airborne spray drift parameter (WT_V=77.20%).

592

593 **5. Conclusions**

594 In this work, spray drift was evaluated under field conditions using the ISO 22866:2005
595 methodology for four 3D crops (peach, citrus, apple and grape) in plots in the EU Southern
596 Zone, comparing STN and DRN nozzles. In all the crops tested, the DRN proved to be an
597 effective and practical technique for the reduction of airborne and sedimenting spray drift.

598 Subsequently, an approach to an initial 3D crop spray drift model was developed and adapted to
599 the conditions of Southern Europe, for both nozzle types. Buffer zones were determined on the
600 basis of these models. The crop growth stage variable was found to be an important factor in the
601 generation of spray drift and must be taken into account when building the models.

602 Finally, a new methodology was defined and tested to evaluate spray drift in field conditions
603 using a LiDAR system. This new methodology, based on scanning the spray drift cloud in the
604 vertical plane, was found to be a practical and effective method for the characterization and
605 determination of DPR in a variety of situations.

606 In future work, progress needs to be made in the generation of a robust model which can be
607 used by the relevant authorities to determine buffer zone dimensions in 3D crops taking into
608 account the main parameters of influence in spray drift. To achieve this result, additional tests
609 will have to be carried out in different scenarios (crops and plots), configurations (sprayers, air
610 assistance, nozzles and operating conditions) and weather conditions. The availability of a new
611 LiDAR methodology for spray drift evaluation, with significant advantages in terms of
612 monitoring and cost, will be crucial to carry out this broad experimental campaign.

613

614 **Acknowledgements**

615 This work was partly funded by the Secretaria d'Universitats i Recerca del Departament
616 d'Empresa i Coneixement de la Generalitat de Catalunya, the Spanish Ministry of Economy and
617 Competitiveness and the European Regional Development Fund (ERDF) under Grants 2017
618 SGR 646, AGL2007-66093-C04-03, AGL2010-22304-04-C03-03, and AGL2013-48297-C2-2-
619 R. The authors also wish to thank Mr. Antonio Checa (Randex Iberica, S.L.) for giving us free
620 Albuz nozzles for the spray tests. Universitat de Lleida is also thanked for Mr. X. Torrent's pre-
621 doctoral fellowship.

622

623 **References**

624 Blanco, M.N., Fenske, R.A, Kasner, E.J., Yost, M.G, Seto, E., Austin, E., 2019. Real-time
625 monitoring of spray drift from three different orchard sprayers. Chemosphere 222, 46-55.
626 https://doi.org/10.1016/j.chemosphere.2019.01.092.

627 Bourodimos, G., Koutsiaras, M., Psiroukis, V., Balafoutis, A., Fountas, S., 2019. Development
628 and field evaluation of a spray drift risk assessment tool for vineyard spraying application.
629 Agriculture 9, 181. https://doi.org/10.3390/agriculture9080181.

630 Butler Ellis, M.C., Lane, A.G., O'Sullivan, C.M.,Miller, P.C.H., Glass, C.R., 2010. Bystander
631 exposure to pesticide spray drift: new data for model development and validation. Biosyst.
632 Eng. 107, 162–168. http://doi.org/10.1016/j.biosystemseng.2010.05.017.

633 Butler Ellis, M.C., Kennedy, M.C., Kuster, C.J., Alanis, R., Tuck, C.R., 2018. Improvements in
634 modelling bystander and resident exposure to pesticide spray drift: Investigation into new
635 approaches for characterizing the collection efficiency of the human body. Ann. Work
636 Expos. Health 62 (5), 622-632. https://doi.org/10.1093/annweh/wxy017.

637 Carlsen, S.C.K., Spliid, N.H., Svensmark, B., 2006. Drift of 10 herbicides after tractor spray
638 application. 2. Primary drift (droplet drift). Chemosphere 64, 778–786.
639 http://doi.org/10.1016/j.chemosphere.2005.10.060.

640 Castro-Tanzi, S., Padilla, L., Brausch, J., Winchell, M., Hanzas, J., 2018. Estimating appropriate
641 buffer distances to mitigate environmental risk of spray drift using field data and computer
642 automation. Abstracts of papers of the 256th National Meeting and Exposition of the
643 American-Chemical-Society (ACS), Boston, MA.

644 Cunha, J.P., Chueca, P., Garcerá, C., Moltó, E., 2012. Risk assessment of pesticide spray drift
645 from citrus application with air-blast sprayers in Spain. Crop Prot. 42, 116–123.
646 http://doi.org/10.1016/j.cropro.2012.06.001.

647 Damalas, Christos A., 2015. Chapter 15. Pesticide drift: Seeking reliable environmental
648 indicators of exposure assessment. In: Armon, R.H., Hanninen, O. (Eds.), Environmental
649 Indicators. Springer Publishing Company, the Netherlands, pp. 251–264.

650 Da Silva, A., Sinfort, C., Tinet, C., Pierrot, D., Huberson, S., 2006. A Lagrangian model for
651 spray behaviour within vine canopies. Aerosol Sci. 37, 658-674.
652 https://doi.org/10.1016/j.jaerosci.2005.05.016.

653 Derksen, R.C., Zhu, H., Fox, R.D., Brazee, R.D., Krause, C.R., 2007. Coverage and drift
654 produced by air induction and conventional hydraulic nozzles used for orchard
655 applications. Trans. ASABE 50 (5), 1493–1501.

656 De Schampheleire, M., Spanoghe, P., Brusselman, E., Sonck, S., 2007. Risk assessment of
657 pesticide spray drift damage in Belgium. Crop Prot. 26, 602–611. http://doi.org/
658 10.1016/j.cropro.2006.05.013.

659 Duga, A.T., Delele, M.A., Ruysen, K., Dekeyser, D., Nuyttens, D., Bylemans, D., Nicolai,
660 B.M., Verboven, P., 2017. Development and validation of 3D CFD model of drift and its
661 application to air-assisted orchard sprayers. Biosyst. Eng. 154, 62-75.
662 http://doi.org/10.1016/j.biosystemseng.2016.10.010.

663 EPA - United States Environmental Protection Agency, 2018. Introduction to pesticide drift
664 [WWW document]. URL. https://www.epa.gov/reducing-pesticide-drift/introduction-
665 pesticide-drift, Access date: 18 August 2018.

666 EPPO (European and Mediterranean Plant Protection Organization), 2003. Environmental risk
667 assessment scheme for plant protection products. Chapter 9: non-target terrestrial
668 arthropods. Bulletin EPPO 33, 99–101.

669 European Union, 2009. Directive 2009/128/EC of the European Parliament and of the Council
670 of 21 October 2009 establishing a framework for Community action to achieve the
671 sustainable use of pesticides. Off. J. Eur. Union 309, 71–86 of 24/11/2009.

672 Eurostat, 2016. Eurostat-Database [online]. Available in:
673 https://ec.europa.eu/eurostat/data/database [Access date: September 10th 2019].

674 Ganzelmeier, H., Rautmann, D., Spangenberg, R., Streloke, M., Herrmann, M., Wenzelburger,
675 H.J., 1995. Studies on the Spray Drift of Plant Protection Products. Blackwell
676 Wissenschafts, Verlag GmbH, Berlin.

677 Garcerá, C., Moltó, E., Chueca, P., 2017. Spray pesticide applications in Mediterranean citrus
678 orchards: canopy deposition and off-target losses. Sci. Total Environ. 599-600, 1344–1362.
679 https://doi.org/10.1016/j.scitotenv.2017.05.029.

680 Gil, E., Llorens, J., Llop, J., Fàbregas, X., Gallart, M., 2013. Use of a terrestrial LiDAR sensor
681 for drift detection in vineyard spraying. Sensors 13 (1), 516-534.
682 https://doi.org/10.3390/s130100516.

683 Gil, Y., Sinfort, C., Brunet, Y., Polveche, V., Bonicelli, B., 2007. Atmospheric loss of pesticides
684 above an artificial vineyard during air-assisted spraying. Atmos. Environ. 41, 2945-2957.
685 https://doi.org/10.1016/j.atmosenv.2006.12.019.

686 Gregorio, E., Rosell-Polo, J.R., Sanz, R., Rocadenbosch, F., Solanelles, F., Garcerà, C., Chueca,
687 P., Arnó, J., del Moral, I., Masip, J., Camp, F., Viana, R., Escolà, A., Gràcia, F., Planas, S.,
688 Moltó, E., 2014. LIDAR as an alternative to passive collectors to measure pesticide spray
689 drift. Atmos. Environ. 82, 83–93. https://doi.org/10.1016/j.atmosenv.2013.09.028.

690 Gregorio, E., Rocadenbosch, F., Sanz, R., Rosell-Polo, J.R., 2015. Eye-Safe lidar system for
691 pesticide spray drift measurement. Sensors (Switzerland) 15, 3650-3670.
692 https://doi.org/10.3390/s150203650.

693 Gregorio, E., Torrent, X., Planas, S., Solanelles, F., Sanz, R., Rocadenbosch, F., Masip, J.,
694 Ribes-Dasi, M., Rosell-Polo, J.R., 2016. Measurement of spray drift with a specifically
695 designed lidar system. Sensors 16(4), 499. https://doi.org/10.3390/s16040499.

696 Gregorio, E., Torrent, X., Planas, S., Rosell-Polo, J.R., 2019. Assessment of spray drift potential
697 reduction for hollow-cone nozzles: Part 2. LiDAR-technique. Sci. Total Environ. 687, 967-
698 977. https://doi.org/ 10.1016/j.scitotenv.2019.06.151.

699 Hiscox, A.L., Miller, D.R., Nappo, C.J., Ross, J., 2006. Dispersion of fine spray from aerial
700 applications in stable atmospheric conditions. Trans. ASABE 49 (5), 1513-1520.

701 Holterman, H.J., van de Zande, J.C., Huijsmans, J.F.M., Wenneker, M., 2017. An empirical
702 model based on phenological growth stage for predicting pesticide spray drift in pome fruit
703 orchards. Biosyst. Eng. 154, 46–61. https://doi.org/10.1016/j.biosystemseng.2016.08.016.

704 ISO 22866, 2005. Equipment for Crop Protection - Methods for Field Measurement of Spray
705 Drift. International Organization for Standardization. Geneva, Switzerland.

706 Kasner, E.J., Fenske, R.A., Hoheisel, G.A., Galvin, K., Blanco, M.N., Seto, E.Y.W., 2018.
707 Spray drift from conventional axial fan airblast sprayer in a modern orchard work
708 environment. Ann. Work Expo. Health 62 (9), 1134-1146.
709 https://doi.org/10.1093/annweh/wxy082.

710 Kira, O., Dubowski, Y., Linker, R., 2018. In-situ open path FTIR measurements of the vertical
711 profile of spray drift from air-assisted sprayers. Biosyst. Eng. 169, 32-41.
712 https://doi.org/10.1016/j.biosystemseng.2018.01.010.

713 Lešnik, M., Stajnko, D., Vajs, S., 2015. Interactions between spray drift and sprayer travel
714 speed in two different apple orchard training systems. Int. J. Environ. Sci. Technol. 12,
715 3017–3028. https://doi.org/10.1007/s13762-014-0724-7.

716 Muscutt, A.D., Harris, G.L., Bailey, S.W., Davies, B.D., 1993. Buffer zones to improve water
717 quality: a review of their potential use in UK agriculture. Agric. Ecosyst.Environ. 45 (1–2),
718 59–77.

719 Nuyttens, D., Sonck, B., de Schampheleire, M., Steurbaut, W., Baetens, K., Verboven, P.,
720 Nicolaï, B., Ramon, H., 2005. Spray drift as affected by meteorological conditions.
721 Commun. Agric. Appl. Biol. Sci. 70, 947–959.

722 Nuyttens, D., De Schampheleire, M., Verboven, P., Sonck, B., 2010. Comparison between
723 indirect and direct spray drift assessment methods. Biosyst. Eng. 105, 2–12. https://
724 doi.org/10.1016/j.biosystemseng.2009.08.004.

725 Ramos, C., Carbonell, G., Baudín, García, Ma, J., Tarazona, J.V., 2000. Ecological risk
726 assessment of pesticides in the Mediterranean region. The need for crop-specific scenarios.
727 Sci. Total Environ. 247, 269–278.

728 Rautmann, D., Streloke, M., Winkler, R., 2001. New basic drift values in the authorisation
729 procedure for plant protection products. In: Forster, R., Streloke, M. (Eds.), Workshop on
730 Risk Assessment and Risk Mitigation Measures in the Context of the Authorisation of
731 Plant Protection Products (WORMM). Mitt. Biol. Bundesanst. Land-Forstwirtsch, Berlin,
732 pp. 133-141.

733 Richardson, B., Strand, T., Thistle, H.W., Hiscox, A., Kimberley, M.O., Schou, W.C., 2017.
734 Influence of a young pinus radiata canopy on aerial spray drift. Trans. ASABE 60 (6),
735 1851-1861. https://doi.org/10.13031/trans.12497.

736 Salyani, M., Miller, D.R., Farooq, M., Sweeb, R.D., 2013. Effects of sprayer operating
737 parameters on airborne drift from citrus air-carrier sprayers. Agric. Eng. Int. CIGR J. 15
738 (1), 27-36. www.cigrjournal.org.

739 Sanz, R., Llorens, J., Escolà, A., Arnó, J., Planas, S., Román, C., Rosell-Polo, J.R., 2018.
740 LIDAR and non-LIDAR-based canopy parameters to estimate the leaf area in fruit trees
741 and vineyard. Agric. For. Meteorol. 260-261, 229-239.
742 https://doi.org/10.1016/j.agrformet.2018.06.017.

743 Sarigiannis, D.A., Kontoroupis, P., Solomou, E.S., Nikolaki, S., Karabelas, A.J., 2013.
744 Inventory of pesticide emissions into the air in Europe. Atmos. Environ. 75, 6-14.
745 http://doi.org/10.1016/j.atmosenv.2013.04.003.

746 Sjerps, R.M.A., Kooij, P.J.F., Van Loon, A., Van Wezel, A.P., 2019. Occurrence of pesticides
747 in Dutch drinking water sources. Chemosphere 235, 510-518.
748 https://doi.org/10.1016/j.chemosphere.2019.06.207.

749 Stainier, C., Destain, M.F., Schiffers, B., Lebeu, F., 2006. Droplet size spectra and drift effect of
750 two phenmedipham formulations and four adjuvants mixtures. Crop Prot. 25, 1238-1243.
751 https://doi.org/10.1016/j.cropro.2006.03.006.

752 Torrent, X., Garcerá, C., Moltó, E., Chueca, P., Abad, R., Grafulla, C., Román, C., Planas, S.,
753 2017. Comparison between standard and drift reducing nozzles for pesticide application in
754 citrus: Part I. effects on wind tunnel and field spray drift. Crop Prot. 96, 130–143.
755 https://doi.org/10.1016/j.cropro.2017.02.001.

756 Torrent, X., Gregorio, E., Douzals, J.P., Tinet, C., Rosell-Polo, J.R., Planas, S., 2019.
757 Assessment of spray drift potential reduction for hollow-cone nozzles: Part 1.
758 Classification using indirect methods. Sci. Total Environ. 692, 1322-1333.
759 https://doi.org/10.1016/j.scitotenv.2019.06.121.

760 Van de Zande, J.C., Stallinga, H., Michielsen, J.M.G.P., van Velde, P., 2010. Effect of width of
761 spray-free buffer zones, nozzle type and air assistance on spray drift. Asp. Appl. Biol.: Int.
762 Adv. Pestic. Appl. 99, 255–263.

763 Wandinger, U., 2005. Introduction to Lidar, in: Weitkamp, C. (Ed.), Lidar. Range-Resolved
764 Optical Remote Sensing of the Atmosphere. Springer-Verlag, pp. 1–18.
765 https://doi.org/10.1007/0-387-25101-4_1.

766 Wenneker, M., van de Zande, J.C., Michielsen, J.M.G.P., Stallinga, H., van Velde, P., 2016.
767 Spray deposition and spray drift in orchard spraying by multiple row sprayers. International
768 advances in pesticide application. Asp. Appl. Biol. 132, 137–144.

769 Wolters, A., Linnemann, V., van de Zande, J.C., Vereecken, H., 2008. Field experiment on
770 spray drift: Deposition and airborne drift during application to a winter wheat crop. Sci.
771 Total Environ. 405, 269-277. https://doi.org/10.1016/j.scitotenv.2008.06.060.

Credit Author Statement

Xavier Torrent: Conceptualization, Methodology, Software, Investigation, Formal analysis, Data curation, Writing - Original Draft, Writing - Review & Editing
Eduard Gregorio: Conceptualization, Methodology, Software, Investigation, Formal analysis, Writing - Original Draft, Writing - Review & Editing, Supervision
Joan R. Rosell-Polo: Conceptualization, Methodology, Investigation, Writing - Review & Editing, Supervision, Funding acquisition
Jaume Arnó: Software, Formal analysis, Writing - Original Draft, Writing - Review & Editing.
Miquel Peris: Investigation, Writing - Review & Editing
Jan C. van de Zande: Investigation, Writing - Review & Editing
Santiago Planas: Conceptualization, Methodology, Investigation, Writing - Review & Editing, Supervision